3B2v8.06a/w (Dec 5 2003).51c + model | JQSRT : 2648 | Prod.Type:FTP pp.1–8(col.fig.:NIL) | ED:R.JothiL. PAGN:vs SCAN:v4soft

ARTICLE IN PRESS

ELSEVIER

Journal of Quantitative Spectroscopy & Radiative Transfer ■ (■■■■) ■■■–■■■

Journal of Quantitative Spectroscopy & Radiative Transfer

www.elsevier.com/locate/jqsrt

Methane diode laser overtone spectroscopy at 840 nm

A. Lucchesini*, S. Gozzini

Istituto per i Processi Chimico-Fisici del CNR, Area della Ricerca, Via G. Moruzzi, 1, I-56124 Pisa, Italy

Received 23 November 2005; accepted 6 February 2006

Abstract

Overtone absorption lines of $^{12}CH_4$ have been examined by using a tunable diode laser (TDL) spectrometer in the region around 11 900 cm^{-1} (840 nm) where the combination overtone band $\nu_1 + 3\nu_3$ lies. The spectrometer sources are commercially available heterostructure GaAlAs TDLs operating in the "free-running" mode, which allowed the detection of the line positions within 0.01 cm^{-1}. The wavelength modulation spectroscopy (WMS) and the second harmonic detection technique permitted the measurements of minimum absorbances of the order of $\simeq 5 \times 10^{-6}$. This allowed to observe the weakest lines of the band with absorption cross-sections of the order of $\simeq 2 \times 10^{-25}$ cm^2/molecule or $\simeq 0.5\,km^{-1}$/amagat. For some of them self-, air-, He- and H_2-broadening coefficients have been obtained at room temperature.

Keywords: Methane absorption coefficients; Overtone bands; Tunable diode-laser spectrometer

1. Introduction

The $^{12}CH_4$ overtones resonances have been detected in the spectra of the outer planets like Uranus, Neptune, Jupiter, Saturn and relative satellites, in particular Titan, therefore the knowledge of the methane absorption features and their behavior with pressure is of crucial importance for mapping the atmospheres. In spite of their weakness, overtone and combination tone absorptions are observable in the absorbing layers of the planets because these are much thicker than the ones obtainable in the laboratory. For example the nice albedo spectrophotometry measurements made by Karkoschka in 1993 [1] at the European Southern Observatory show clearly the methane overtones of the visible e.m. spectrum in the jovian planets and also in Titanus.

Intensity measurements in the visible and in the near infrared have been systematically performed in the past by conventional spectroscopy by analyzing the telescope photographic plates [2] or by using long path White cells in the laboratories [3,4]. More recently, in order to detect the weak combination overtone bands, O'Brien and Cao [5] took advantage of the intracavity laser spectroscopy (ILS) technique by a sophisticated spectroscopic apparatus.

*Corresponding author. Fax: +39 0503152 230.
E-mail address: lucchesini@ipcf.cnr.it (A. Lucchesini).

0022-4073/$ - see front matter © 2006 Published by Elsevier Ltd.
doi:10.1016/j.jqsrt.2006.02.056

Here we present a spectroscopic work based on the use of the semiconductor diode lasers (DLs), inexpensive radiation sources still suitable for high-resolution spectroscopy even without any external optical and electrical feedback (*free-running*). Basing on one of the more interesting properties of the DLs, that is the modulability through the injection current, we employed the frequency modulation (FM) technique [6] with the purpose of increasing the signal-to-noise ratio (S/N); this is a necessity when dealing with very weak absorption resonances like the overtones or the combination tones.

When the value of the frequency is chosen much lower than the resonance line-width, the FM spectroscopy is usually called "wavelength modulation spectroscopy" (WMS). In this work, we apply the WMS and the second harmonic detection to methane around 840 nm, where the CH_4 combination overtone band $\nu_1 + 3\nu_3$ is located.

2. Experimental setup

Fig. 1 shows the experimental setup adopted for the WMS. The source is a Fabry–Perot-type semiconductor laser Roithner Lasertechnik Mod. RLT85100G that emits up to 100 mW single mode at 847 nm without any external optical feedback, that is in *free-running* mode. It is driven by a stabilized low-noise current supply. Its temperature is monitored by a high-stability controller ($\Delta T = 0.01$ K within 1 h). The temperature control of the DL is very important as its emission wavelength is a linear function of the temperature (≈ 0.1 nm/K) with periodical mode hops. The wavelength scan is obtained by adding a low-frequency ($\sim$1 Hz) sawtooth signal to the driving current. The wavelength dependence on the current is linear for small current variations (≈ 0.01 nm/mA, the influence of the quadratic component is less than 10^{-4} nm/mA) and is a critical parameter for free-running DL spectroscopy (usual current amplitudes range 10–100 mA). The collimated DL radiation is split in 4 different beams; the first passes through a confocal 5 cm Fabry–Perot interferometer to check the frequency sweep and the laser emission mode; two beams go through two Herriott-type multipass cells 30 m path length each, one containing the sample gas and the other containing water vapor for checking whether the obtained absorption features come from H_2O as expected (see HITRAN database [7]); finally one laser beam passes through an iodine reference cell for the precise wavenumber measurements. The transmitted radiations are collected by pre-amplified silicon photodiodes and the resulting signals are simultaneously

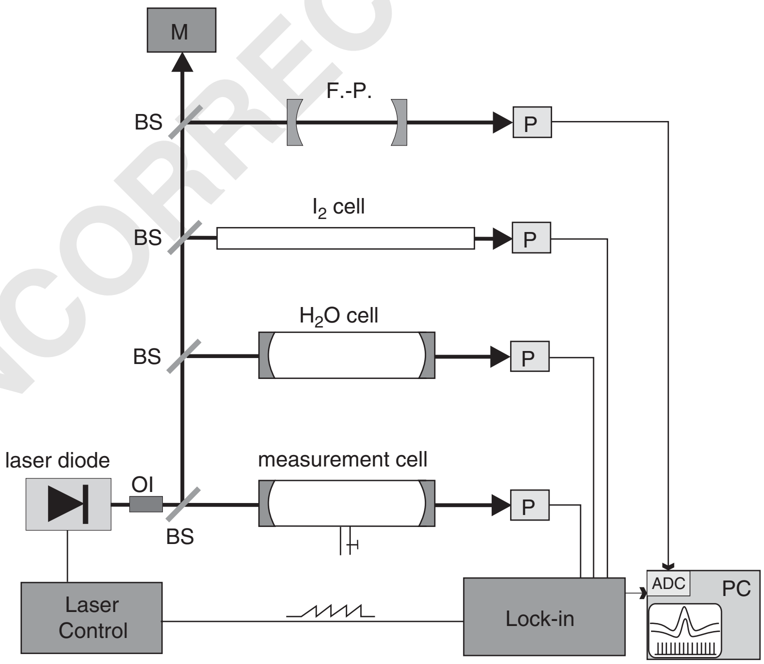

Fig. 1. Outline of the experimental apparatus. BS: beam splitter; F.–P.: Fabry–Perot interferometer; M: monochromator; OI: optical insulator; P: photodiode; PC: desk-top computer.

acquired by a desk-top computer via a National Instruments Lab-PC 12-bit analog-to-digital converter (ADC). A 35 cm focal length monochromator is employed for the rough wavelength reading ($\Delta\lambda \simeq 0.01$ nm). A sinusoidal current is mixed to the DL injection current for the harmonic detection: the signals transmitted through the cells are sent to the lock-in amplifiers to extract the desired harmonic components. An optical insulator is put in front of the DL in order to avoid the "feedback noise" due to the reflections coming from the various optical elements along the beam path. The methane gas was supplied by Praxair Inc. with the following nominal characteristics: grade 5.5 (purity$\geqslant$99.9995%), $H_2O \leqslant 2$ ppmv,$O_2 \leq 0.5$ ppmv, $N_2 \leq 10$ ppmv, $H_2O \leqslant 0.1$ ppmv. For accurate pressure measurements in our ranges (from 20 to 300 torr) we used a capacitive gauge Varian Mod. 6543-25-045.

3. Frequency modulation

We describe the intensity of the radiation after passing through a sample as the product of the incoming intensity $I_0(v)$ and the transmittance $\tau(v)$, where v is the distance from the central frequency of the line:

$$I(v) = I_0(v)\tau(v). \tag{1}$$

The transmittance in its turn is described by the Lambert–Beer equation:

$$\tau(v) = e^{-\sigma(v)\,z}, \tag{2}$$

where $z = \rho\, l$ is the column amount (in molecule/cm^2), i.e. the product of the absorbing species number density ρ (in molecule/cm^3) and the optical path l (in cm) of the radiation through the sample; the absorption cross-section $\sigma(v)$ is expressed in cm^2/molecule. In case of small optical depths [$\sigma(v)z \ll 1$], which is always verified in our case, Eq. (2) can be approximated by

$$\tau(v) \simeq 1 - \sigma(v)\,z. \tag{3}$$

$\sigma(v)$ must take into account the shape of the absorption line: Gaussian-like for Doppler broadening and Lorentzian-like for collisional broadening.

In our measurement conditions other effects like the Dicke narrowing that occurs when the molecular mean free path is comparable to the wavelength of the radiation [8], are not significantly observed and are not taken into account. In this scenario, to describe well the absorption coefficient as a function of the radiation frequency is the Voigt function [9], that is the convolution of the Lorentz and the Gauss curves:

$$f(v) = \int_{-\infty}^{+\infty} \frac{\exp[-(t - v_o)^2/\Gamma_G^2 \ln 2]}{(t - v)^2 + \Gamma_L^2}\, dt, \tag{4}$$

where v_o is the gas resonance frequency, Γ_G and Γ_L are the Gaussian and the Lorentzian half-widths at half-maximum (HWHM), respectively.

When FM is used, the emission frequency of the DL is sinusoidally modulated at frequency $v_m = \omega_m/2\pi$ via the injection current,

$$v = \bar{v} + a \cos \omega_m t. \tag{5}$$

If the DL emission frequency $\bar{v}$ is swept over an interval across the chosen transition, one gets a signal that depends on both the line shape and the modulation parameters. Since it is an even function of the time, it can be written as a cosine Fourier series,

$$\tau(\bar{v} + a \cos \omega_m t) = \sum_{n=0}^{\infty} H_n(\bar{v}, a) \cos n\omega_m t, \tag{6}$$

where $H_n(\bar{v})$ is the nth harmonic component of the modulated signal. By demodulating the signal with a lock-in amplifier at a multiple nv_m ($n = 1, 2, \ldots$) of the modulation frequency, an output signal that is proportional to the nth component $H_n(\bar{v})$ is collected. When the amplitude a is chosen smaller than the width of the transition line, the nth Fourier component is proportional to the n-order derivative of the original signal,

$$H_n(\bar{\nu}, a) = \frac{2^{1-n}}{n!}\, a^n \left.\frac{\mathrm{d}^n \tau(\nu)}{\mathrm{d}\nu^n}\right|_{\nu=\bar{\nu}}, \quad n \geqslant 1. \tag{7}$$

During this work we used a low modulation amplitude and we detected the second harmonic component (*2f detection*), which enhanced the S/N ratio and reduced to zero the unwanted background. In order to extract the line parameters, we used a nonlinear least-squares fit procedure explained elsewhere [10]. In particular, to obtain the collisional (pressure) broadening coefficients we fitted the full-width at half-maximum (FWHM) γ_L vs. pressure by the general expression:

$$\gamma_\mathrm{L}(p) = 2\Gamma_\mathrm{L}(p) = \gamma_i p_i + \gamma_\mathrm{self} p_o, \tag{8}$$

where γ_i is the FWHM broadening coefficient related to the i buffer gas, p_i is the buffer gas partial pressure, γ_self is the sample gas FWHM self-broadening coefficient and p_o is the sample gas partial pressure.

4. Experimental results

During this work 48 absorption lines have been observed and their position measured within 0.01 cm^{-1} by the comparison with a very precisely known I_2 absorption spectrum [11] coming from an I_2 reference cell. Table 1 shows the results with the wavenumbers (ν') in vacuum. The listed wavelengths are in air at 294 K and have been deduced by using the index of refraction formula from the work of Edlén [12]. They presumably belong to the combination overtone band $\nu_1 + 3\nu_3$ [3], where ν_1 is the symmetric stretch and ν_3 is the asymmetric stretch fundamental vibration.

Ought to the derivative spectroscopy method adopted here it is difficult to obtain absolute intensity measurements directly from the *2f* signals. We tried to measure the absolute transmission values by using the direct absorption (DA) technique at room temperature (RT) on the same path-length as the one adopted with WMS and with a CH_4 pressure around 95–100 torr, which gives the best S/N. The maximum absorption cross-

Table 1
List of the observed CH_4 lines along with the maximum absorption cross-section

λ at 294 K (nm)	ν' (cm^{-1})	σ_max (10^{-24} cm^2/molecule)	λ at 294 K (nm)	ν' (cm^{-1})	σ_max (10^{-24} cm^2/molecule)
838.180	11 927.40	2.84	841.894	11 874.78	0.75
838.208	11 927.00	0.74	843.364	11 854.09	0.60
838.214	11 926.92	0.65	843.384	11 853.80	1.04
838.219	11 926.84	1.16	843.400	11 853.58	0.25
838.269	11 926.13		843.452	11 852.85	1.30
838.477	11 923.17	1.14	843.495	11 852.25	0.53
838.755	11 919.23	0.76	843.852	11 847.23	0.94
839.058	11 914.92	3.27	843.869	11 846.99	0.61
839.066	11 914.81		8443.57	11 840.15	1.71
839.076	11 914.66	1.57	844.748	11 834.67	0.37
839.955	11 902.20	0.78	844.757	11 834.54	1.01
839.963	11 902.08	1.14	845.063	11 830.25	1.26
839.972	11 901.95	1.19	845.077	11 830.06	0.56
840.087	11 900.33	0.80	845.080	11 830.01	
840.123	11 899.82		845.629	11 822.33	0.52
840.242	11 898.13	1.19	845.654	11 821.99	0.53
840.262	11 897.85	0.74	845.668	11 821.79	0.48
840.289	11 897.47	0.81	845.677	11 821.67	
841.038	11 886.87	1.40	845.685	11 821.55	
841.056	11 886.61		845.701	11 821.33	
841.178	11 884.89	2.38	845.716	11 821.12	
841.658	11 878.12	0.43	845.737	11 820.83	1.55
841.721	11 877.22	1.71	845.748	11 820.67	0.62
841.840	11 875.55	0.78	846.696	11 807.44	0.21

sections shown in the table for most of the lines are obtained by this way, and the measurement errors could not be better than approximately 10%.

An example of the spectrum as obtained by WMS and the second derivative technique is shown in Fig. 2, where four methane lines are extracted by the fit procedure. When dealing with free-running DLs, a frequency sweep of their emission is always associated with a variation of the emission intensity, therefore in Fig. 2 the relative intensity ratios does not give the real ratios, but modified by this intensity change. In particular in this case, when moving the LD emission wavenumber by $-1\,\mathrm{cm}^{-1}$, the LD emission intensity increased by 3.8 times.

The complexity of the structure of the $v_1 + 3v_3$ band does not permit an immediate and correct quantum classification of the ro-vibrational resonances. For these highly excited levels the numerous possible resonances between ro-vibrational levels can modify significantly the intensity as well as the position of the expected lines. Tentatively, basing upon the intensity distribution, the lines within $(11\,807.44 \leq v' \leq 11\,854.09)\,\mathrm{cm}^{-1}$ should belong to the P branch, the ones within $(11\,874.78 \leqslant v' \leq 11\,886.87)\,\mathrm{cm}^{-1}$ to the Q branch and the lines in between $(11\,897.47 \leqslant v' \leqslant 11\,927.40)\,\mathrm{cm}^{-1}$ to the R branch.

4.1. Line broadening and shifting measurements

Table 2 shows the measured CH_4 pressure broadening coefficients by itself, air, H_2 and He gases, all at RT for some of the more intense observed lines. The shown errors are the maximum errors (3σ).

In order to obtain the pressure shift coefficients we acquired simultaneously the CH_4 and I_2 absorptions from their respective measurements cells, taking the latter at fixed pressure and temperature for reference; sometimes we used H_2O at fixed pressure at RT in its cell as the reference.

Examples of pressure broadening and shifting measurements are in Figs. 3 and 4, where CH_4 broadening and shifting behaviors by collision with itself and helium buffer gas are displayed, respectively, with their best linear fit.

For the 840 nm band there are no previous pressure broadening and shifting measurements therefore a comparison can be done only with the results on different wavelengths. Moreover ought to the lack of quantum assignment of the lines in this band, only an average comparison can be done. Most of our broadening coefficients at RT in average are a little lower than the ones coming from previous works on $2v_3$-overtone [13,14]. The same happens for the self- and the H_2-broadening [15], for He- and H_2-broadening for

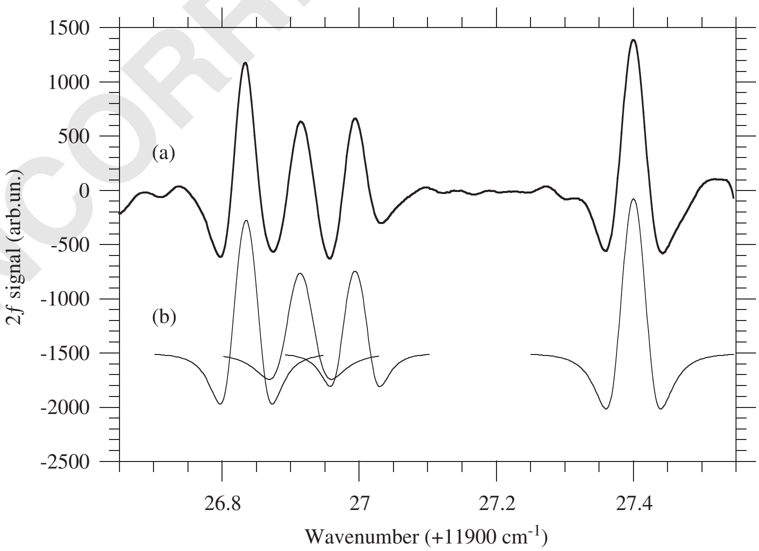

Fig. 2. Second derivative signal of the methane transmission spectrum around 838.2 nm (a) obtained by WMS with 10 Hz bandwidth at $p_{CH_4} = 95$ torr and $T = 296$ K. The peaks extracted by the fit procedure (b) are shifted down for clearness.

Table 2
Methane pressure broadening FWHM coefficients (γ) at room temperature

ν' (cm^{-1})	γ_{self} (MHz/torr)	γ_{air} (MHz/torr)	γ_{H2} (MHz/torr)	γ_{He} (MHz/torr)
11 914.92	6.4 ± 0.2	4.5 ± 0.2	4.8 ± 0.1	3.6 ± 0.1
11 898.13	6.1 ± 0.1	3.4 ± 0.2	4.8 ± 0.2	3.4 ± 0.2
11 897.85	5.4 ± 0.7	3.4 ± 0.4	3.6 ± 0.5	3.0 ± 0.8
11 886.87	6.4 ± 0.1	4.4 ± 0.4	5.0 ± 0.2	3.7 ± 0.3
11 853.80	6.5 ± 0.1	6.2 ± 0.3	4.8 ± 0.2	3.6 ± 0.3
11 847.23	8.7 ± 0.2	6.3 ± 0.6	8.5 ± 0.2	3.8 ± 0.9
11 840.15	5.2 ± 0.1	3.7 ± 0.3	4.9 ± 0.2	3.2 ± 0.1

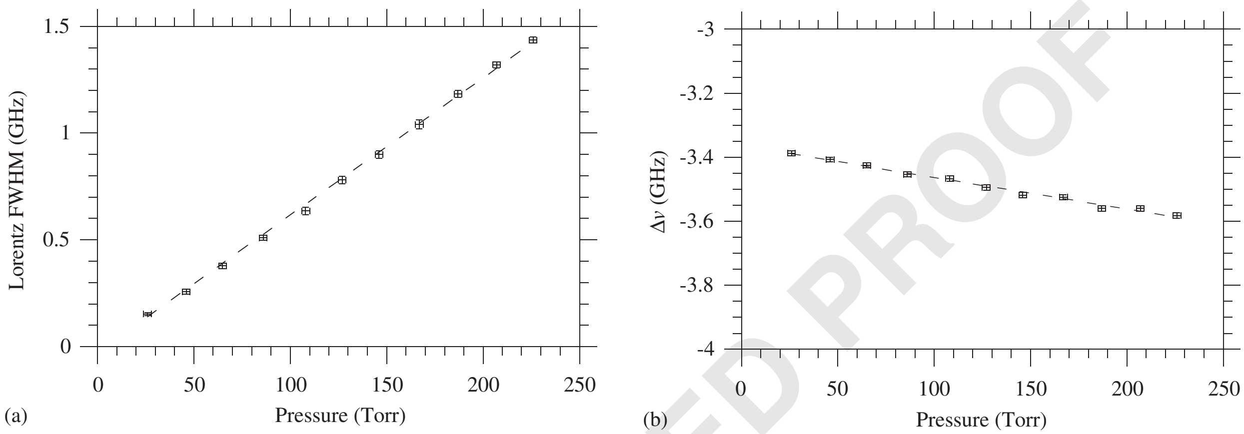

Fig. 3. Variation of the Lorentz width (a) and of the relative line position $\Delta\nu$ (b) in GHz of the 11 886.87 cm^{-1} absorption line as a function of CH_4 pressure at room temperature.

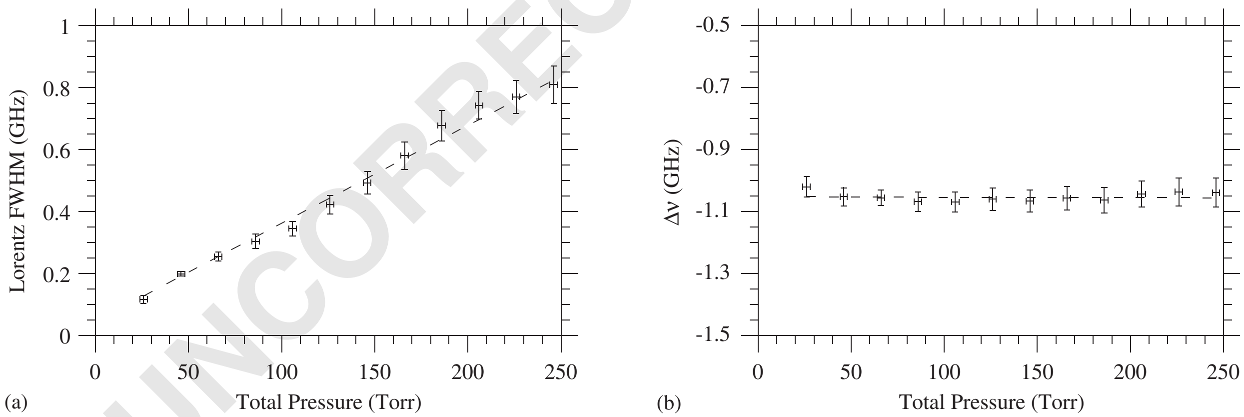

Fig. 4. He-broadening (a) and -shifting (b) measurements for the 11 840.15 cm^{-1} methane absorption line (room temperature).

the $3\nu_3$ overtone band [16] and for the air-broadened ν_3-fundamental [17], while there are no much differences in the H_2- and He-broadening measurements on the ν_4-fundamental [18] at RT. As already said, our system has not enough sensitivity to estimate the contribution of an eventual Dicke narrowing, but this phenomenon could explain some of these differences.

The summary of the measured pressure shift coefficients is shown in Table 3. The air-shift coefficients are in average roughly 10 times higher than the ones got by others on the fundamentals ν_2 and ν_4 [19] and very much dependent on the lines.

Table 3
Methane pressure shift coefficients (δ) at room temperature

ν' (cm^{-1})	δ_{self} (MHz/torr)	δ_{air} (MHz/torr)	δ_{H_2} (MHz/torr)	δ_{He} (MHz/torr)
11 914.92	-1.3 ± 0.3	-1.1 ± 0.1	-0.7 ± 0.3	0.3 ± 0.1
11 898.13	-1.1 ± 0.1	-0.6 ± 0.1	-0.6 ± 0.1	-0.2 ± 0.1
11 897.85	-1.4 ± 0.2	-0.9 ± 0.1	-0.7 ± 0.1	0.4 ± 0.3
11 886.87	-1.0 ± 0.1	-0.5 ± 0.1	-0.8 ± 0.1	0.1 ± 0.3
11 853.80	-0.9 ± 0.1	-0.7 ± 0.1	-0.9 ± 0.1	0.0 ± 0.1
11 847.23	-0.3 ± 0.4	-0.8 ± 0.3	-0.4 ± 0.3	0.1 ± 0.3
11 840.15	-1.5 ± 0.1	-0.9 ± 0.1	-0.8 ± 0.1	0.0 ± 0.2

Very recently Predoi-Cross [20] et al. measured the self-broadening and shift coefficients in laboratory by using the McMath–Pierce Fourier transform spectrometer of the Kitt Peak National Solar Observatory in the $\nu_1 + \nu_4$, $\nu_3 + \nu_4$ and $\nu_2 + \nu_3$ combination tone bands of $^{12}CH_4$: while the self-broadenings are quite the same, the self-shifts are two or three times lower than ours. The same happens in the comparison with the recent work on the $\nu_2 + \nu_4$ combination band made by Mondelain et al. [21]. These big differences are noted also in the air- and He-shifts on the R3 triplet in the $2\nu_3$ band by Zèninari et al. [14], where in particular they show a linear dependence of the air-induced shift with the energy of the upper vibrational state: this occurs because the shift value depends on the vibrational quantum numbers as well as the polarizability of the perturbing element [22].

5. Conclusion

By diode laser WM spectroscopy with high resolving power ($\lambda/\Delta\lambda \approx 10^7$) and the aid of a 30 m total path-length multipass Herriott-type measurement cell, 48 CH_4 absorption lines have been detected around 11 900 cm^{-1} and their positions measured within 0.01 cm^{-1}. They presumably belong to the combination overtone $\nu_1 + 3\nu_3$ ro-vibrational band. The absolute line positions have been obtained by comparison with a reference I_2 absorption cell and the utilization of a very precise atlas. The maximum absorption cross section of the observed lines ranges between 2×10^{-25} and 3×10^{-24} cm^2/molecule at RT. Collisional broadening and shift coefficients for different perturbing gases have been measured at RT for 7 of the more intense absorption lines.

Acknowledgments

The authors wish to thank Mr. M. Badalassi for the realization of the I_2 reference cell, Mr. R. Ripoli for the mechanical set up and Mr. Mauro Tagliaferri for the technical assistance. Special thanks go to Prof. G. Alzetta and to Dr. D. Bertolini for their encouragement and suggestions.

References

[1] Karkoschka E. Spectrophotometry of the Jovian planets and Titan at 300- to 1000-nm wavelength: the methane spectrum. Icarus 1994;111:174–92.
[2] Vedder H, Mecke A. Das Rotationsschwingungsspectrum des methans. Z Phys 1933;86:137–56.
[3] Giver LP. Intensity measurements of the CH_4 bands in the region 4350 to 10 600 Å. JQSRT 1978;19:311–22.
[4] Dick KA, Fink U. Photoelectric absorption spectra of methane (CH_4), methane and hydrogen (H_2) mixtures, and ethane (C_2H_6). JQSRT 1977;18:433–46.
[5] O'Brien JJ, Cao H. Absorption spectra and absorption coefficients for methane in the 750–940 nm region obtained by intracavity laser spectroscopy. JQSRT 2002;75:323–50.
[6] Bjorklund GC. Frequency-modulation spectroscopy: a new method for measuring weak absorptions and dispersions. Opt Lett 1980;5:15–7.
[7] Rothman LS, Jacquemart D, Barbe A, Chris Benner D, Birk M, Brown LR, Carleer MR, Chackerian Jr C, Chance K, Coudert LH, Dana V, Devi VM, Flaud J-M, Gamache RR, Goldman A, Hartmann J-M, Jucks KW, Maki AG, Mandin J-Y, Massie ST, Orphal J,

Perrin A, Rinsland CP, Smith MAH, Tennyson J, Tolchenov RN, Toth RA, Vander Auwera J, Varanasi P, Wagner G. The HITRAN 2004 molecular spectroscopic database. JQSRT 2005;96:139–204.

[8] Dicke RH. The effect of collision upon the Doppler width of the spectral lines. Phys Rev 1953;89:472–3.

[9] Armstrong BH. Spectrum line profile: the Voigt function. JQSRT 1967;7:61–88.

[10] De Rosa M, Ciucci A, Pelliccia D, Gabbanini C, Gozzini S, Lucchesini A. On the measurement of pressure induced shift by diode lasers and harmonic detection. Opt Commun 1998;147:55–60.

[11] Gerstenkorn S, Verges S, Chevillard J. Atlas du spectre d'absorption de la molécule d'iode. Lab, Aimé Cotton, Orsay, France: Edition du CNRS; 1982.

[12] Edlén B. The refractive index of air. Metrologia 1966;2:71–80.

[13] Varanasi P. Collision-broadened half-widths and shapes of methane lines. JQSRT 1971;11:1711–24.

[14] Zéninari V, Parvitte B, Curtuois D, Kapitanov VA, Ponomarev YuN. Measurements of air and noble-gas broadening and shift coefficients of the methane R3 triplet of the $2\nu_3$ band. Appl Phys B 2001;72:953–9

Zéninari V, Parvitte B, Courtois D, Kapitanov V, Ponomarev YuN. Study of the methane broadening and shift coefficients by the atmospheric gases pressure: air, O_2, N_2 and H_2. In: Poster H15 presented at the 16th international conference on high resolution molecular spectroscopy, PRAHA2000, Prague, Czech Republic, September 3–7, 2000.

[15] Fink U, Benner DC, Dick KA. Band model analysis of laboratory methane absorption spectra from 4500 to 10 500 Å. JQSRT 1977;18:447–57.

[16] Fox K, Jennings DE, Stern EA, Hubbard R. Measurements of argon-, helium-, hydrogen-, and nitrogen-broadened widths of methane lines near $9000\,cm^{-1}$. JQSRT 1988;39:473–6.

[17] Varanasi P. Air-broadened line widths of methane at atmospheric temperature. JQSRT 1974;15:281.

[18] Varanasi P. Measurements of collision-broadened line widths in the ν_4-fundamental band of $^{12}CH_4$ at low temperatures. JQSRT 1989;41:335–43.

[19] Rinsland CP, Malathy Devi V, Smith MAH, Benner DC. Measurements of air-broadened and nitrogen-broadened Lorentz width coefficients and pressure shift coefficients in the ν_4 and ν_2 bands of $^{12}CH_4$. Appl Opt 1988;27:631–51.

[20] Predoi-Cross A, Brown LR, Malathy Devi V, Brawley-Tremblay M, Benner DC. Multispectrum analysis of $^{12}CH_4$ from 4100 to $4635\,cm^{-1}$, 1: self-broadening coefficients (widths and shifts). J Mol Spectrosc 2005;232:231–46.

[21] Mondelain D, Chelin P, Valentin A, Hurtmans D, Camy-Peret C. Line profile study by diode laser spectroscopy in the $^{12}CH_4$ $\nu_2 + \nu_4$ band. J Mol Spectrosc 2005;233:23–31.

[22] Lazarev VV, Ponomarev YuN, Sumpf B, Fleischmann O, Waschull J, Kronfeldt H-D, Stroinova VN. Noble gas pressure-induced broadening and shift of H_2O and SO_2 absorption lines. J Mol Spectrosc 1995;173:177–93.